





# An Energy-aware Dynamic Data Allocation Mechanism for Many-channel Memory Systems

Masayuki Sato<sup>1</sup> , Takuya Toyoshima<sup>1</sup>, Hikaru Takayashiki<sup>1</sup> ,  
Ryusuke Egawa<sup>1</sup> , Hiroaki Kobayashi<sup>1</sup> 

© The Authors 2019. This paper is published with open access at SuperFri.org

A modern memory system is equipped with many memory channels to obtain a high memory bandwidth. To take the advantage of this organization, applications' data are distributed among the channels and transferred in an interleaved fashion. Although memory-intensive applications benefit from a high bandwidth by many memory channels, applications such as compute-intensive ones do not need the high bandwidth. To reduce the energy consumption for such applications, the memory system has *low-power modes*. During no memory request, the main memory can enter these modes and reduce energy consumption. However, these applications often cause intermittent memory requests to the channels that handle their data, resulting in not entering the low-power modes. Hence, the memory system cannot enter the low-power modes even though the applications do not need the high bandwidth. To solve this problem, this paper proposes a dynamic data allocation mechanism for many-channel memory systems. This mechanism forces data of such applications to use the specified channels by dynamically changing the address-mapping schemes and migrating the data. As a result, the other channels to which the data are not allocated can have a chance to enter the low-power modes for a long time. Therefore, the proposed mechanism has the potential to reduce the energy consumption of many-channel memory systems. The evaluation results show that this mechanism can reduce the energy consumption by up to 11.8% and 1.7% on average.

*Keywords:* DRAM, main memory, low-power mode, address-mapping scheme, energy consumption.

## Introduction

Modern microprocessors have improved their performances by increasing the numbers of cores significantly [3]. As a result, a high memory bandwidth is required by a microprocessor and applications executed on it [16]. On the other hand, the speed of Dynamic Random Access Memory (DRAM), which is used as a main memory, has modestly improved. Due to the performance gap between microprocessors and main memories, the main memories cannot supply the data at enough speed to the microprocessor. Therefore, a main memory has been a bottleneck in the performance of a modern computing system. This problem is well-known as the “Memory Wall” problem [18].

To cope with such a situation, the latest computing systems have a main memory system with many memory channels to obtain the higher memory bandwidth. Such a *many-channel memory system* is widely employed in industrial microprocessors from personal computers to supercomputer systems. For example, a memory module with 3D-integration technologies, High Bandwidth Memory (HBM), has 8 channels physically, and can act as a 16-channel module in the pseudo-channel mode [13]. Since six HBM modules can be integrated with a microprocessor on a silicon interposer [19], it is possible for a single memory system to have 48 to 96 channels.

On the other hand, not all applications require such a high memory bandwidth. As the diversity among applications increases, the applications could be categorized into memory-intensive and compute-intensive applications. The compute-intensive applications do not always need high bandwidths. For these applications, such a high bandwidth memory has a little performance im-

---

<sup>1</sup>Tohoku University, Sendai, Japan

pact and causes a high energy consumption. To reduce the energy consumption of the memory system in compute-intensive applications, DRAM-based memory systems have several low-power modes. These modes can reduce the power consumption by deactivating peripheral circuits of DRAM chips when the compute-intensive applications do not need the memory performance.

However, to take the advantages of using many channels simultaneously and get their full bandwidth, the data of an application are distributed among all the memory channels in an interleaved fashion, determined by *an address-mapping scheme*. Since the data placement for any applications is treated under a single address-mapping scheme, the data of the compute-intensive applications are also distributed. If these applications intermittently cause memory requests to all the channels, memory systems cannot enter the low-power modes, although they do not need to use the whole bandwidth. Therefore, address-mapping schemes should be appropriately selected so that the memory system can reduce the energy consumption by aggressively using the low-power modes.

To solve this problem, this paper proposes an energy-aware dynamic data allocation mechanism for many-channel memory systems. This mechanism dynamically switches two address-mapping schemes based on the access frequencies. One scheme is to distribute the data among channels, and the other scheme is to gather the data into specific memory channels. When the applications do not need to use all of the channels for the highest bandwidth, this mechanism selects the scheme that gathers the data accessed frequently into limited memory channels. By selecting this scheme, the access frequencies to the other channels can be reduced, and these channels can get more opportunities to enter the low-power modes. Therefore, this mechanism has the potential to reduce the energy consumption of many-channel memory systems. Note that, if the proposed mechanism switches the address-mapping schemes without caring the data, a memory system cannot correctly provide the data that are stored based on the address-mapping scheme used before the switching. To avoid such a situation, the proposed mechanism migrates data stored by the previous scheme so that they can be accessed by the current scheme. Therefore, the proposed mechanism can continue to correctly process the memory requests.

The rest of this paper is organized as follows. Section 1 explains the low-power modes and discusses the effectiveness of the low-power modes. Section 2 discusses address-mapping schemes to change the number of accessed channels, and proposes a dynamic mechanism that changes these schemes during an execution to reflect the demand for the memory bandwidth of applications. Section 3 shows the evaluation results that support the effectiveness of the proposed mechanism. The final section concludes this paper.

## 1. Power Management of Memory Systems

### 1.1. Basic Organization of a DRAM-based Memory System

Figure 1 shows a block diagram of a typical DRAM-based memory system. The system consists of channels, ranks, bank groups, and banks hierarchically. Note that the existence of these hierarchical layers and the number of components in each layer depend on the DRAM standards and the configuration of the memory system [7, 11]. A single channel contains some ranks, and each rank can be selected by chip-select lines and/or chip-ID lines. The rank selected by these lines accepts the commands on the shared buses. Each rank contains banks that are arrays of DRAM cells, or sometimes bank groups, which are groups of multiple banks. In each bank, DRAM cells are organized by rows and columns in DRAM arrays. The DRAM array is

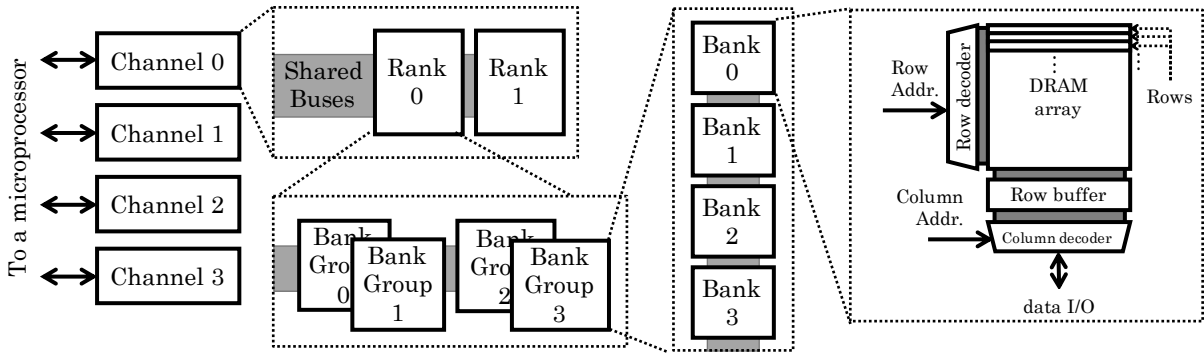


Figure 1. Overview of a memory system

accompanied by peripheral circuits to read/write data from/to a single row, and provide data in columns to the microprocessor.

The procedure to access the data is summarized in the following three steps. All the commands for these steps pass through the shared buses. The first step is *precharge*. This step sets up banks that include the accessed data. In this step, a row buffer adjoining each bank is cleared with writing its data back to the DRAM cells, and the banks and their peripheral circuits are prepared for the next step. The next step is *row activation*. In this step, one of the rows in the bank is specified by the row decoder, and then the data in the row are read out to the row buffer. The third step is *column read/write*. In this step, the column in the row buffer is specified. In the case of a read request, the column data are read out from the row buffer to the shared data bus. In the case of a write request, the data sent from the shared bus are stored in the target column in the row buffer.

To access the data based on these steps, it is requested to determine which bank, row, column, and rank should be accessed. To this end, the physical address included in a memory request is used. From the bit sequence of the physical address, the IDs of these hierarchical components are extracted as subsets of the bit sequence. A rule that determines how these IDs are taken from the physical address is called an *address-mapping scheme*.

## 1.2. Low-power Mode

Figure 2 shows the state transition diagram of a DRAM chip. Each state corresponds to each mode that the DRAM chip can transit. Idle mode is an initial state. If a bank receives the row-activation command (ACT), the bank transits to the state *active*. In this state, the bank can accept read/write operations issued by the column read and write commands. On the other hand, when the bank receives the precharge command (PRE), the state of the bank returns to idle. In the case where all the banks in the rank become the Idle state and receive the refresh command (REF), the rank starts to refresh data to avoid the DRAM cells from losing the data by leakage current.

For reducing the energy consumption of DRAM-based memory systems, the DRAM standards include the low-power modes. A rank can enter the low-power mode under the conditions that there is no waiting command based on the memory request to the banks, and the rank receives command *PDX* or *SRX*. As shown in Fig. 2, there are several low-power modes, e.g., the active power-down mode, the precharge power-down mode, and the self-refresh mode. The mode that the rank can enter is different depending on the original state. The deeper low-power mode is more effective to reduce the power consumption.

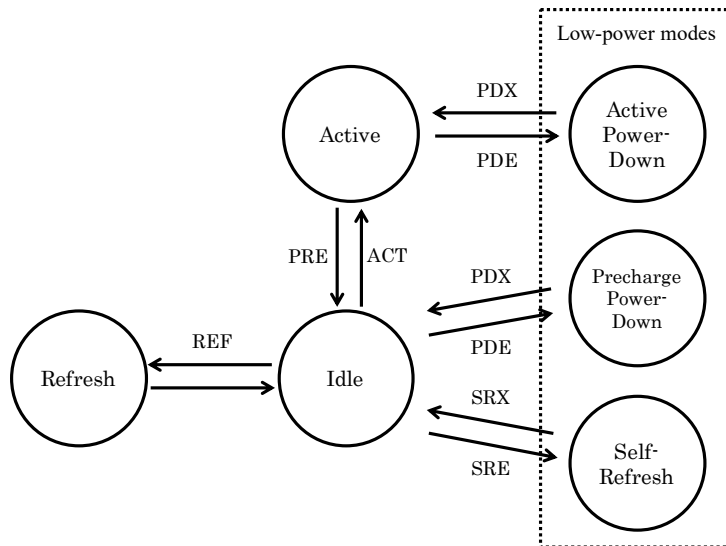


Figure 2. State transition diagram of power modes

### 1.3. Limitation of the Deep Low-power Mode

To reduce the power consumption of the memory system, the low-power mode should be appropriately used. This is because the energy consumption may increase due to the latency for the recovery from the low-power modes to the active mode. To obtain the target data in the rank in the low-power modes, the memory requests have to wait for the recovery of the ranks from the low-power modes. The recovery process needs to enable the power supply for the disabled circuits, resulting in a certain latency. If accesses invoke the recovery process frequently, the accumulated latency may cause a significant performance penalty for the executed application. As a result, the execution time of the application and the energy consumption may increase even if the power consumption decreases. Among the three low-power modes, the self-refresh mode is the most effective to reduce the power consumption, but the recovery latency is also the largest among them, which results in the large performance penalty [14].

To evaluate how the low-power modes, especially the self-refresh mode, can be exploited in a modern memory system, the preliminary evaluation is conducted by simulation. The target system has a 4GB HBM2 memory module for the main memory. The detailed parameters of the system are shown in Tab. 1. The latency parameters of HBM2 refer to [4], and the current parameters are based on those of a DDR4 module that has the same voltage and clock frequency [11]. In this simulation, the gem5 simulator system [1] is used. Applications executed on the simulator are selected from the SPEC CPU2006 benchmark suite. Each application is executed by three billion instructions after skipping the first one billion instructions.

The details of the self-refresh mode are as follows. Generally, to suppress the performance penalty, the rank can enter the self-refresh mode after a certain idle period has continued. In addition, one normal refresh operation should be done before moving to the self-refresh mode [11]. Therefore, in this simulation experiment, the rank enters the self-refresh mode after the conditions that a certain period without access is elapsed, and one refresh operation completes. The period is empirically determined as 78,000 cycles so that the performance degradation due to the self-refresh mode becomes less than 1%.

Figure 3 shows the evaluation results of the usage of the self-refresh mode. The left vertical axis and the bar graphs show a ratio of time in the self-refresh mode to the total execution time.

Table 1. Simulation parameters

Core	4GHz, 8 instruction width, out-of-order
L1 I-cache	8 ways, 32KB, 2-cycles latency
L1 D-cache	8 ways, 32KB, 2-cycles latency
L2 cache	8 ways, 1MB, 20-cycles latency
Main memory	HBM2, 4GB, 8 channels

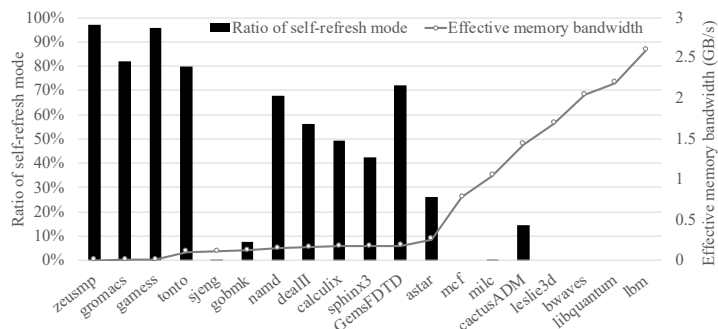
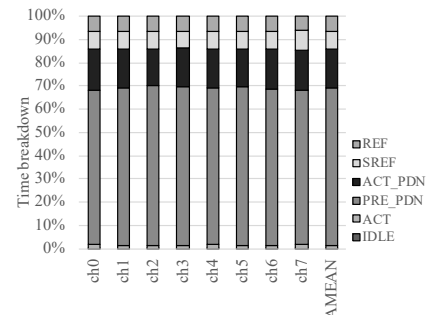


Figure 3. Ratio of self-refresh mode and effective memory bandwidth


 Figure 4. Ratio of times in various modes to the total time (*gobmk\_13x13*)

The right vertical axis and the line graph indicate the effective memory bandwidth in the case without the self-refresh mode. All of these values are averaged by those of all the eight channels. Figure 3 shows the trend that the ratio of the self-refresh mode becomes smaller as the sustained memory bandwidth increases. This trend is very intuitive. As the number of memory requests increases, the idle time between a request and its subsequent one becomes shorter. Hence, the memory system cannot easily enter the self-refresh mode.

Focusing on each benchmark, the ratios of the self-refresh mode in some benchmarks are very low, 0.08% in *sjeng* and 7.8% in *gobmk*, respectively. Each of the benchmarks cannot enter the self-refresh mode at all while its effective bandwidth is low enough compared with the other applications. To more deeply discuss this fact, Fig. 4 shows the breakdown of the total execution time into times for individual modes in *gobmk*. This graph shows the results of all the channels. Figure 4 shows that the ratio of the self-refresh mode (*SREF*) to the total time is only 8%. In contrast, the precharge power-down mode (*PRE\_PDN*) is dominant. This fact means that the time duration between one request and the subsequent request is long enough to enter the precharge power-down mode but too short to enter the self-refresh mode. This situation occurs for all the channels. Therefore, these results indicate that it is difficult to fully exploit the self-refresh mode for the applications that cause memory requests intermittently.

#### 1.4. Related Work

This section reviews the related work to reduce the power and energy consumption of the DRAM-based memory systems.

Weis *et al.* [15] have proposed a physical interface that can reduce the energy consumption instead of decreasing the memory bandwidth. This proposal focuses on some applications that cannot exploit the bigger bus width. Therefore, they divide a bus into multiple sub-buses and enables a memory array to activate only a part of a row. This research focuses on the dynamic energy on fine-grain data access pattern, not on the effective usage of the low-power modes.

While this paper focuses on power management using channels, there are some studies focusing on power management using memory ranks. Lebeck *et al.* [9] have discussed how to effectively use DRAM chips including the low-power modes. They have investigated the parameters to enter the low-power modes, and show the first preliminary results of the frequency-based page allocation, which determines the page allocation based on the access frequency. Wu *et al.* have proposed *RAMZzz* [17]. Because applications generally have different access locality, *RAMZzz* dynamically migrates the memory pages, which are accessed frequently, into some of the ranks. Since the other ranks store only the pages that are less accessed, these ranks can obtain more room to enter the low-power mode. Jang *et al.* [8] have proposed a rank-aware power management method considering the virtual machines to reduce the memory power consumption of data centers. This work considers the scheduling of virtual machines and the placement of their data on the memory system together. The data of virtual machines that are simultaneously executed in multiple cores are gathered into the same memory ranks. Sato *et al.* [12] have proposed a rank-based power management method using multiple address-mapping schemes. Each of the address-mapping schemes determines how data with a physical address is mapped to a physical position of a DRAM-based memory system. By changing the address-mapping schemes, the proposal can gather the data into a single rank or distribute the data across multiple ranks regardless of applications and virtual machines. However, the address-mapping schemes have the limitations, and this method cannot exploit all the ranks to increase the performance.

One of the potential problems of these four studies mentioned above is that the power/energy management is done by controlling ranks. These proposals can work on a memory system with multiple ranks and becomes effective as the number of ranks increases. On the other hand, there are systems that have only one rank in reality. For example, there are typical cases that a personal computer has two DIMM modules, each of which has one rank. However, these modules are generally used for increasing the number of channels for performance improvement, not for increasing the number of ranks per channel. Moreover, the latest high-performance memory module, HBM2, has 8 channels but only one rank [13]. In such cases, the rank-based power management methods cannot be applied.

Hur *et al.* have proposed the *adaptive memory throttling* [6]. This method purposely blocks the incoming memory commands during a certain period. By delaying the commands, the memory system can increase the idle time. The number of cycles for blocking is determined by access history to suppress performance degradation. Bojnordi *et al.* have proposed the programmable memory controller, *PARDIS* [2]. This controller has a dedicated instruction set architecture for accessing DDR memories. They also have implemented application-specific address-mapping schemes on *PARDIS* and have succeeded in improving the performance and reducing the energy consumption. This fact supports that the memory controller should adopt the deeper optimization regarding the address-mapping schemes. Although these studies do not focus on adjusting the number of requests to ranks and channels, these approaches can be combined with those exploiting the low-power modes by reducing the number of requests.

From the above discussions, this paper focuses on reducing the energy consumption by effective usage of the built-in self-refresh modes and finding an alternative of the rank-based power management methods. There are many cases that the number of ranks is limited in a single memory system. Therefore, this paper focuses on *channels*, which are alternatives to ranks to gather or distribute the data. If the data are gathered into one channel, the number of memory requests to the other channels can be reduced, and the ranks in these channels can

enter the self-refresh mode regardless of the number of ranks. Such an approach will become requisite in the era of many-channel memory systems.

## 2. Energy-aware Data Placement for Many-channel Memory Systems

### 2.1. Exploiting the Low-power Modes

Compute-intensive applications do not require the high bandwidth realized by many channels because their access requests are intermittent and not frequent. However, as shown in the results in Section 1.3, some of compute-intensive applications cannot exploit the low-power modes. These applications' data are distributed to all the channels, and these intermittent requests to the data also widely spread over the channels. The frequency of these requests is small but not enough to allow the channels and their components to enter the self-refresh modes. Therefore, the energy consumption of the memory system increases even in the case of compute-intensive applications.

Figure 5 shows the concept of our approach to solve the above problem. Figure 5a is a mode that can fully use all the channels, the *full-channel mode*. In this mode, the applications' data are distributed to all the eight channels. In this mode, the memory system can achieve the highest memory bandwidth. On the other hand, Fig. 5b is a mode that can use a limited number of channels. In this case, all the data are stored into Channels 0 and 1, and only these channels are accessed. To realize such a situation, the data in Channels 2 to 7 are migrated to Channels 0 and 1. Then, Channels 2 to 7 are not accessed. Therefore, these channels can move to the self-refresh mode. The compute-intensive applications can keep the high performance even though the memory system with limited channels reduces the bandwidth.

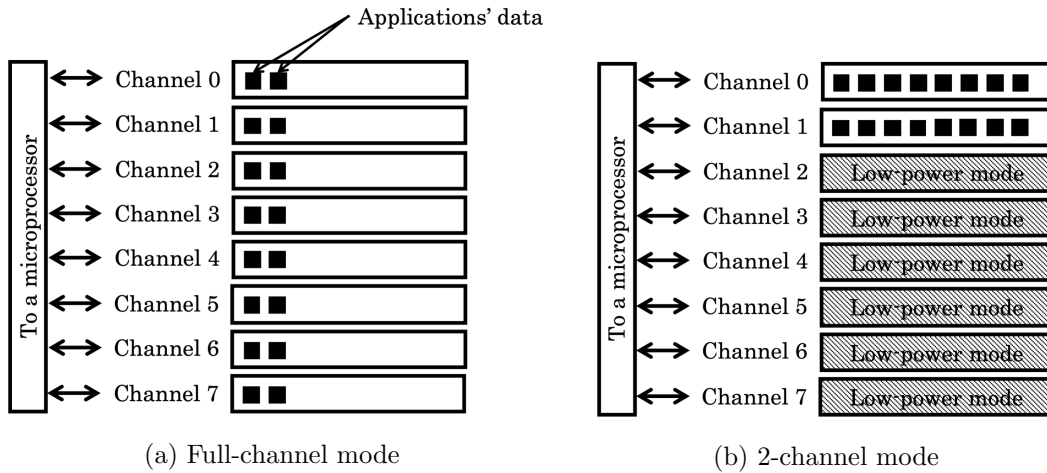


**Figure 5.** Full-channel mode for high performance and 2-channel mode for low power

To control different channel modes, this paper considers using address-mapping schemes. As mentioned in Section 1.4, an address-mapping scheme determines where data with a physical address is mapped to a physical location in the DRAM-based memory system. Therefore, each channel mode can be realized by an address-mapping scheme. If these address-mapping schemes can be switched, it can change the channel modes. To switch the address-mapping schemes, the locations of the data of the old scheme can be easily known by those of the new schemes.

This is because, when switching the schemes, the data stored in the memory system have to be migrated to the locations mapped by the newly-switched scheme.

To satisfy the above conditions, this paper considers variations of address-mapping schemes inspired by matrix transposition. By the matrix transpositions, the elements standing in one row are rearranged as those in one column. Such rearranging can be applied to the data migrations to distribute the data over the channels or gather the data into one channel. Figure 6 shows two address-mapping schemes in the case of an 8-channel memory system, and how these schemes map the sequential addresses to channels and groups of rows, called *row groups*. Figure 6a is the scheme for the full-channel mode. Figure 6b is for the 2-channel mode. When the addresses in each scheme are regarded as items in a matrix, those of the 2-channel mode can be generated by transposing those of the full-channel mode by 2x2 sub-matrices. The orange and blue areas in the figures show where the 2x2 sub-matrices are exchanged.

These schemes can satisfy the requirement to realize the channel modes. If the memory requests are based on a sequential access pattern, the requests are distributed, and the accessed channel is changed for each request in Fig. 6a. On the other hand, in the 2-channel mode in Fig. 6b, the sequential access requests firstly go to Channels 0 and 1. After all the data in these channels are accessed, the subsequent requests go to Channels 2 and 3 until all the data in these channels are accessed. Such an access pattern continues to Channels 6 to 7. Focusing on a certain period during execution, two channels are accessed simultaneously. Moreover, to change the channel modes, data are migrated by the pattern of matrix transposition. There is no need to memorize the mapping between physical addresses and locations on the memory system.

	Ch. 0	Ch. 1	Ch. 2	Ch. 3	Ch. 4	Ch. 5	Ch. 6	Ch. 7		Ch. 0	Ch. 1	Ch. 2	Ch. 3	Ch. 4	Ch. 5	Ch. 6	Ch. 7
Row group 0	0	1	2	3	4	5	6	7	Row group 0	0	1	16	17	32	33	48	49
Row group 1	8	9	10	11	12	13	14	15	Row group 1	8	9	24	25	40	41	56	57
Row group 2	16	17	18	19	20	21	22	23	Row group 2	2	3	18	19	34	35	50	51
Row group 3	24	25	26	27	28	29	30	31	Row group 3	10	11	26	27	42	43	58	59
Row group 4	32	33	34	35	36	37	38	39	Row group 4	4	5	20	21	36	37	52	53
Row group 5	40	41	42	43	44	45	46	47	Row group 5	12	13	28	29	44	45	60	61
Row group 6	48	49	50	51	52	53	54	55	Row group 6	6	7	22	23	38	39	54	55
Row group 7	56	57	58	59	60	61	62	63	Row group 7	14	15	30	31	46	47	62	63

(a) Full-channel mode

(b) 2-channel mode

**Figure 6.** Maps of the sequential addresses to the channels and the row groups

Figure 7 shows how a physical address is mapped to the physical location of DRAM. These examples are the cases of switching the full-channel mode and the two-channel mode. In the full-channel mode, the bits of row address, bank address, channel address, and column address are extracted as shown in Fig. 7. The channel address is extracted from the least significant bits except for the column address. In the 2-channel mode, the most significant two bits in the row address are exchanged. Hence, the channel address is generated by using the most significant two bits and the least significant one bit except for the column address. Generally, due to the locality of memory accesses, the lower bits in the physical address are changed easier than the upper bits. Therefore, in the 2-channel mode, the lower one bit of the channel address easily changes, but the upper two bits hardly change. It limits the number of accessed channels to two in a certain period. These address-mapping schemes can be generalized. Here, the number of the lower bits in the channel address is defined as  $n$ . The matrix transposition shown in Fig. 6 is done by  $n \times n$  sub-matrices, and the scheme can limit the number of accessed channels to  $2^n$ .



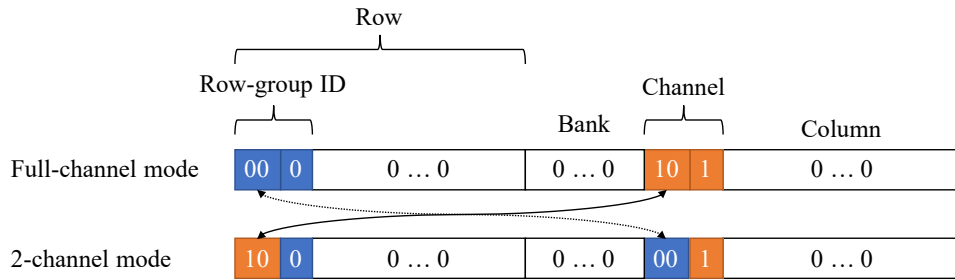


Figure 7. Address-mapping schemes limiting the number of channels

## 2.2. Dynamic Data Allocation Mechanism

### 2.2.1. Hardware organization

To realize switching the channel modes, this paper proposes the dynamic data allocation mechanism. The proposed mechanism is implemented on the memory controller, which is the front-end of accessing the memory system. In the case where the number of channels is large, a lot of channel modes are available, e.g., the 1-channel mode, the 2-channel mode, the 4-channel mode, and the full-channel mode in the case where the number of channels is eight. To suppress the hardware cost to manage these modes, the full-channel mode and another channel mode are considered in this paper.

Figure 8 shows the memory controller with the proposed dynamic data allocation mechanism. The memory controller is accompanied with additional components, the *mode register*, the *mode table*, and the *access counter*. The mode register indicates which channel mode should be used currently. The preferred channel mode is determined by the number of accesses at a certain period. The controller counts memory requests by using the access counter. The mode table manages which channel mode is used for the previous access to the physical address by memorizing pairs of the physical address and its channel mode. Note that, the proposed mechanism migrates the data in a unit of row only when the included data are firstly accessed after switching the schemes. This is because it takes a long time to complete migrating all the data to every switching. Therefore, the mode table has to store the pairs for every row.

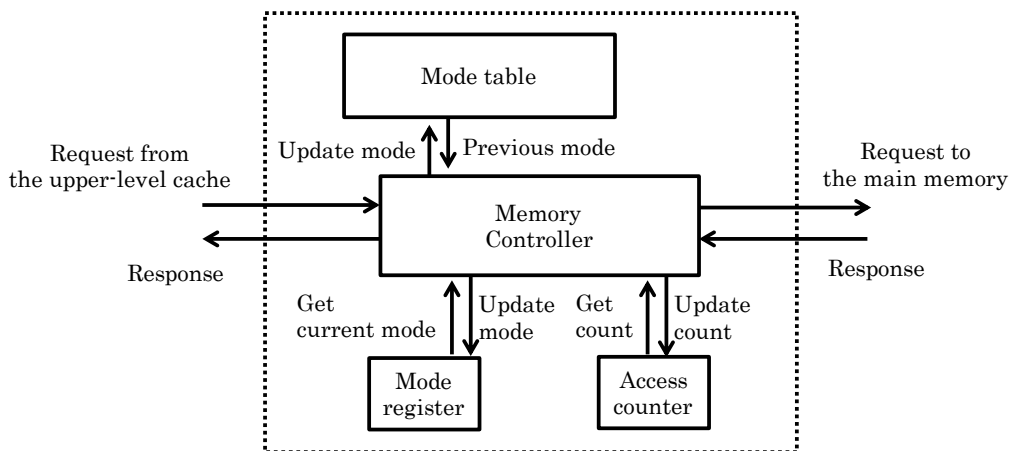


Figure 8. Dynamic data allocation mechanism: a memory controller with facilities switching channel modes

### 2.2.2. Memory access procedure

The memory controller with the proposed mechanism is placed between the processor and the main memory. The address conversion is done only in the lower layers from the memory controller. Therefore, the processor-side hardware does not need to know whether the data are migrated or not. The memory controller determines the physical location of the address of a memory request by the address-mapping scheme currently selected, and processes the access request.

The detailed procedure to process the memory requests is as follows. If a memory request comes from the processor, the controller knows which is the current mode from the mode register. Next, the controller accesses the mode table based on the physical address to know the mode used in the previous access to that address. If the current mode is different from the previous mode, the data are migrated so that the data can be accessed by the current mode. The mode table is also updated to store the current mode for this physical address. Finally, the memory request is processed by the current mode as the normal memory controller does.

After receiving the data from the main memory, the memory controller knows the channel mode from the mode table when the memory request comes. If the mode is changed from the default mode, here the full-channel mode, the data are sent directly to the processor. If the mode is different from the default mode, the address is reverted to the original one, and the data are sent to the processor.

### 2.2.3. Hardware overhead of the mechanism

To realize such a migration mechanism, the mode table needs to store the previous address-mapping scheme for each row. In the case where the controller switches two schemes, the mode table should be indexed by a row address, and each entry should store one bit that indicates the mode. In addition, the rows to be swapped should be kept temporarily for the migrations. These costs depend on the configuration of the memory system. The details of the overhead will be discussed in Section 3.

## 3. Evaluations

### 3.1. Evaluation Setup

#### 3.1.1. Applications

To evaluate the proposed mechanism, both the applications examined in Section 1.3 and multi-programmed workloads, which are generated by randomly selecting four applications as shown in Tab. 2, are used. To understand the effectiveness of the proposal more clearly, the applications and the multi-programmed workloads combining them are categorized based on the effective bandwidth on average. If the effective bandwidth of an application is lower than 0.5GB/s, the application belongs to Category A. If the bandwidth is higher than 0.5GB/s, the application is put into Category B. Note that the effectiveness of the proposal for the above applications and workloads can also be applied to multi-threaded applications. This is because the proposed mechanism can be affected only by the number of accesses per fixed interval but not by any other factors of applications and workloads. As a result, this paper examines the performance by using single-threaded applications and their multi-programmed workloads only.

**Table 2.** Multi-programmed workloads

	Applications	Effective Bandwidth (GB/s)
M1	zeusmp, gromacs, sjeng, gobmk	0.163
M2	zeusmp, gamess, sjeng, namd	0.175
M3	tonto, sjeng, gobmk, namd	0.334
M4	dealII, calculix, sphinx3, GemsFDTD	0.526
M5	gamess, gobmk, calculix, astar	0.777
M6	zeusmp, sjeng, calculix, mcf	1.01
M7	gromacs, gobmk, sphinx3, milc	1.54
M8	gamess, namd, GemsFDTD, cactusADM	1.71
M9	dealII, sphinx3, astar, milc	2.11
M10	calculix, GemsFDTD, mcf, cactusADM	2.55
M11	calculix, sphinx3, bwaves, libquantum	2.65
M12	tonto, calculix, milc, lbm	3.78
M13	astar, mcf, milc, cactusADM	3.82
M14	astar, milc, leslie3d, libquantum	4.13
M15	dealII, GemsFDTD, leslie3d, lbm	4.36
M16	mcf, cactusADM, bwaves, lbm	5.60
M17	leslie3d, bwaves, libquantum, lbm	5.91

### 3.1.2. Parameters of the proposed mechanism

To evaluate the proposed mechanism, the simulation experiment is conducted. This evaluation supposes that the target system has a 4GB HBM2 module with eight channels as the main memory. The simulation parameters are similar to those of the preliminary experiment in Section 1.3, but the system has four cores with L1 private I/D caches, and the L2 cache is shared among the cores. In this experiment, the proposed mechanism switches two schemes, the full-channel mode that uses eight channels and the 2-channel modes. For the proposed scheme, two parameters, *an interval to switch the modes* and *the threshold to trigger the switch*, should be determined. The relationships between these parameters and the effectiveness of the proposal are preliminarily evaluated. Based on the results, the threshold that triggers to switch the mode is set to 0.64GB/s, and the interval to change the scheme is 50ms.

The simulation starts by using the full-channel mode, and the proposed mechanism does not change the initial scheme until the first one billion instructions are skipped. After this skipping, the switching function of the proposed scheme is enabled, and the data correction for the evaluation is validated.

As mentioned in Section 2.2.3, the proposed mechanism needs additional hardware units. The mode table holding which rows are swapped is the most dominant unit from the viewpoint of the energy consumption. In the case of a 4GB memory, the row size of which is 2KB, the mode table has to memorize which channel mode is applied to each row. From this fact, the table should be indexed by 20 bits, and each entry in the table has a one-bit flag that indicates the mode. On the other hand, the table does not need to hold the status of one row for each group of swapped rows and the regions that are not needed to be migrated. By eliminating these status

bits, the number of entries can be reduced by three-eighths. Therefore, the table size required for this experimental condition is 93KB.

The energy overhead of this mode table is estimated by using CACTI [10] and statistics from the simulator. CACTI can estimate the dynamic read and write energy consumptions and the leakage power of memory arrays. Since the number of accesses to the mode table and the execution time can be estimated by the simulator, the total energy consumption of the mode table can be calculated for each workload. Note that the capacity of the memory array must be  $2^n$  bytes in CACTI where  $n$  is a natural number. Therefore, the estimated results of the 128KB SRAM array are used in this evaluation. The technology node and the transistor model used in this evaluation is 22nm and the Low Standby Power model (LSTP), respectively. Since the number of accesses to the mode table is not so large compared with those to the upper-level caches, the LSTP transistor can contribute to the reduction in the total energy consumption of the mode table.

## 3.2. Evaluation Results

### 3.2.1. Performance

In this paper, the performances of the multi-programmed workloads are evaluated by the *weighted speedup* [5]. This metric is defined as Equation (1).

$$\text{WeightedSpeedup} = \sum_i^N \frac{IPC_i^{\text{shared}}}{IPC_i^{\text{alone}}} \quad (1)$$

Here,  $IPC_i^{\text{alone}}$  means IPC of the  $i$ -th application in the case where the  $i$ -th application is executed solely.  $IPC_i^{\text{shared}}$  stands for IPC of that application in the case where the application runs with all the  $N$  applications in the workload together. The higher weighted speedup means the better performance. Moreover, this metric can fairly assess the workload performance even in the case where one application has a large IPC but the others mark lower IPCs.

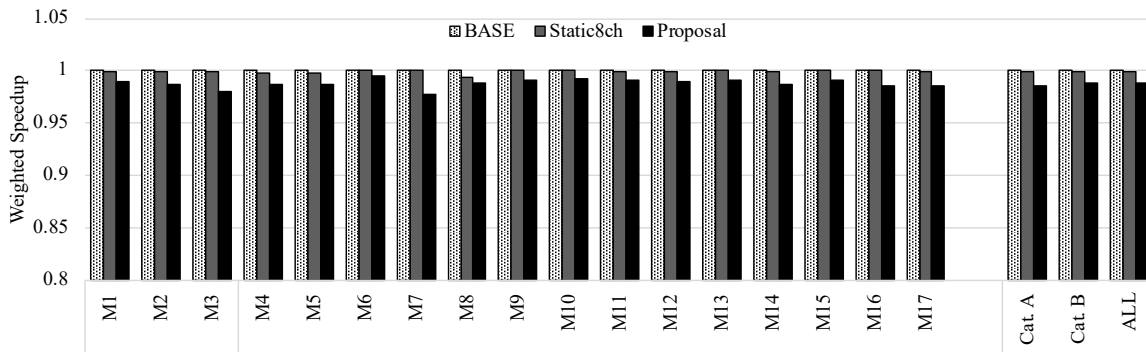


**Figure 9.** Evaluation results of performance

Figure 9 shows the evaluation results of the performance. The horizontal axis shows the workloads used in this evaluation, and the vertical axis shows the weighted speedup when the self-refresh mode is not used, called *BASE*. The four graphs in one application show the performances in the case of *BASE*, *Static8ch* that always uses the full-channel mode, and *Proposal* showing the results of the proposed mechanism.

Figure 9 shows that, on average, the proposed mechanism slightly decreases the performance by up to 2.3% compared with *BASE* and *Static8ch*. Note that these results include the

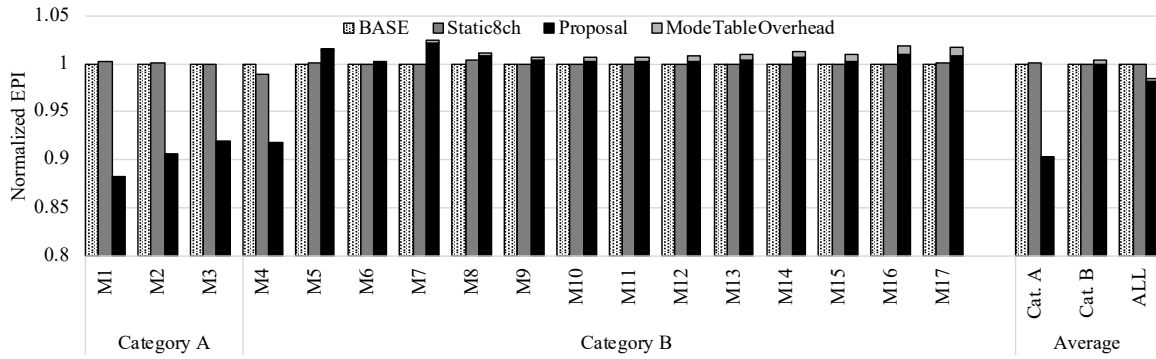


Figure 10. Evaluation results of energy per instruction

performance overheads by the additional latency and the migration costs of the proposed mechanism. Therefore, the performance of the proposed mechanism does not reach those of *BASE* and *Static8ch*.

Comparing the workloads in Category A and those in Category B, there are no remarkable differences. The workloads in the Category A easily switch to the two-channel mode because of the low effective memory bandwidth. Although switching the schemes causes the migration overhead, its performance penalty is not so large compared with those of Category B. Therefore, the impact of the migration overhead of the proposed mechanism on the performance is not significant.

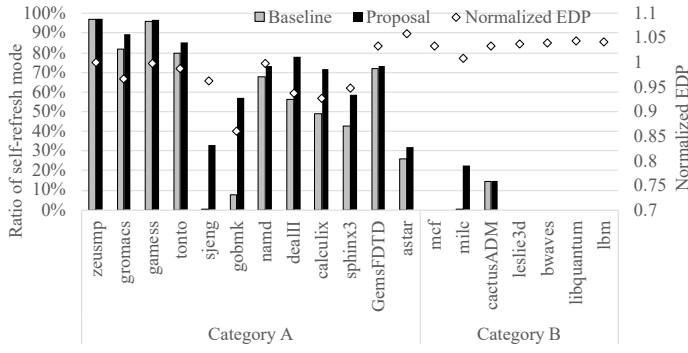
### 3.2.2. Energy consumption

Figure 10 shows the evaluation results of the energy consumptions. The horizontal axis shows the workloads, and the vertical axis shows the energy per instruction (EPI) normalized by the results of *BASE*, which does not use the self-refresh mode. The legend of the graph is almost the same as that of Fig. 9, but an energy overhead of the mode table is added as *ModeTableOverhead*. Note that the energy consumption by the additional memory requests for the migration is already included in that of the proposal.

From Fig. 10, it is observed that the EPIs of the proposed scheme are smaller than those of *BASE* and *Static8ch* on average. The proposed mechanism reduces the EPIs by up to 11.8% and 12.0%, and 1.7% and 1.6% on average compared with *BASE* and *Static8ch*, respectively. Therefore, the proposed mechanism can contribute to the reduction in the energy consumption by reducing the number of channels.

Focusing on each category, the EPIs of the workloads in Category A are reduced by 9.9% on average. It indicates that the proposed mechanism is effective for these applications, each of which marks the lower bandwidth. On the other hand, for the workloads in Category B, the proposed mechanism cannot reduce the EPIs. This is because the proposed mechanism cannot switch to the 2-channel mode to avoid performance degradation for these workloads.

The proposed mechanism causes the energy overheads due to the migration of the data for switching the modes. Their effects on average do not overwhelm the advantage of the proposed mechanism. However, for some workloads, especially M5 and M7, their EPIs slightly increase. During the execution of these workloads, there are some periods where their effective bandwidth becomes lower than 0.5GB/s. The proposed mechanism switches to the 2-channel modes in that period, and it causes additional memory requests for the migration. Moreover, the overheads of the mode table are relatively large in Category B. This is because the mode table has been



**Figure 11.** The ratio of entering the self-refresh mode

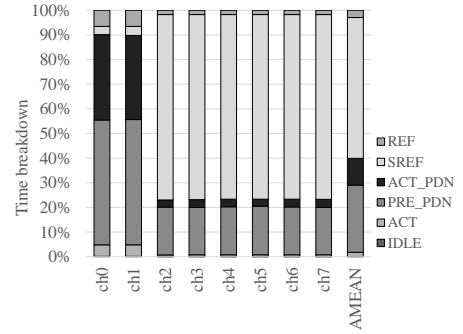


**Figure 12.** Breakdown of the channels in each mode

checked every memory access. Since the benchmarks in Category B need many memory accesses, the number of accesses to the mode table also becomes large. Therefore, the energy consumption of the mode table increases.

### 3.2.3. Mode breakdown

To analyze the effectiveness of the proposed mechanism, this section evaluates the breakdown of the execution time in the single-thread application. Figure 11 shows the total length of the period in the self-refresh mode and their effects. The horizontal axis shows the applications. The left vertical axis and two bar graphs show ratios of the self-refresh mode to the total time. The two graphs show the ratios of *Baseline* and *Proposal*, which are the original address-mapping scheme and the proposed mechanism, respectively. The right vertical axis and dot graphs show the energy-delay products when using the proposed mechanism, which is normalized by that of *Baseline*.

From Fig. 11, it is observed that the ratio of the self-refresh mode increases by the proposed mechanism compared with *Baseline*. This fact indicates that the proposed mechanism actually increases the time in the self-refresh mode, resulting in the energy reduction. The applications, the times of which in the self-refresh mode increase, especially in Category A, can reduce the energy-delay products. Otherwise, in Category B, the energy-delay products do not decrease. As a result, the energy-delay products slightly increase due to the performance degradations by the performance overheads of the proposed mechanism.

Among these applications, the proposed mechanism is most beneficial to the benchmark gobmk. To analyze the details of this application, Fig. 12 shows the breakdown of the total execution time into times for individual modes in gobmk. The difference from Fig. 4 is that the proposed mechanism is applied. From Fig. 12, it is clear that the time in the self-refresh mode increases compared with the case in Fig. 4 in the six channels that are *ch2* to *ch7* in these figures. This is the main reason for reducing the energy consumption. On the other hand, the fact that the ratios of the active mode (*ACT*) increase in *ch0* and *ch1* indicates that the proposed mechanism successfully gathers the frequently accessed data into *ch0* and *ch1*. Although the time durations of the self-refresh mode of these channels decrease, its effect is not dominant for the total energy consumption.

## Conclusions

Modern computing systems employ memory systems with many memory channels to obtain the higher performance. However, the access request comes into the system intermittently, the

ranks in the channels cannot exploit the lower-power modes, especially the self-refresh modes. To solve this problem, this paper proposes a dynamic data allocation mechanism for many-channel memory systems. The proposed mechanism switches multiple address-mapping schemes. One scheme is for limiting the number of accessed channels to reduce the energy consumption. The other scheme is to fully exploit all the channels to obtain the higher performance. The evaluation results show that the proposed mechanism can reduce the energy consumption by up to 11.8% and 1.7% on average.

As future work, the variations of channel modes by different address-mapping schemes should be explored. The proposed mechanism should use more effective channel modes. Furthermore, the proposed mechanism switches only the two modes, however, may become more effective by switching three or more channel modes.

## Acknowledgement

This work is partially supported by MEXT Next Generation High-Performance Computing Infrastructures and Applications R&D Program, entitled “R&D of A Quantum-Annealing-Assisted Next Generation HPC Infrastructure and its Applications” and Grants-in-Aid for Early-Career Scientists No. 19K20232.

*This paper is distributed under the terms of the Creative Commons Attribution-Non Commercial 3.0 License which permits non-commercial use, reproduction and distribution of the work without further permission provided the original work is properly cited.*

## References

1. Binkert, N., Beckmann, B., Black, G., Reinhardt, S.K., Saidi, A., Basu, A., Hestness, J., Hower, D.R., Krishna, T., Sardashti, S., Sen, R., Sewell, K., Shoib, M., Vaish, N., Hill, M.D., Wood, D.A.: The gem5 simulator. ACM SIGARCH Computer Architecture News 39, 1–7 (Aug 2011), DOI: 10.1145/2024716.2024718
2. Bojnordi, M.N., Ipek, E.: Pardis: A programmable memory controller for the DDRx interfacing standards. In: 39th Annual International Symposium on Computer Architecture. pp. 13–24. IEEE, Portland, OR, USA (Jun 2012), DOI: 10.1109/ISCA.2012.6237002
3. Borkar, S.: Thousand core chips: A technology perspective. In: The 44th Annual Design Automation Conference. pp. 746–749. DAC '07, ACM, New York, NY, USA (2007), DOI: 10.1145/1278480.1278667
4. Chatterjee, N., O'Connor, M., Lee, D., Johnson, D.R., Keckler, S.W., Rhu, M., Dally, W.J.: Architecting an energy-efficient DRAM system for GPUs. In: IEEE International Symposium on High Performance Computer Architecture (HPCA). pp. 73–84. Austin, TX, USA (2017), DOI: 10.1109/HPCA.2017.58
5. Eyerman, S., Eeckhout, L.: System-level performance metrics for multiprogram workloads. IEEE Micro 28(3), 42–53 (2008), DOI: 10.1109/MM.2008.44
6. Hur, I., Lin, C.: A comprehensive approach to DRAM power management. In: IEEE 14th International Symposium on High Performance Computer Architecture. pp. 305–316. Salt Lake City, UT, USA (Feb 2008), DOI: 10.1109/HPCA.2008.4658648

7. Jacob, B., Ng, S.W., Wang, D.T.: Memory Systems: Cache, DRAM, Disk. Morgan Kaufmann (2008)
8. Jang, J.W., Jeon, M., Kim, H.S., Jo, H., Kim, J.S., Maeng, S.: Energy reduction in consolidated servers through memory-aware virtual machine scheduling. *Computers, IEEE Transactions on* 60(4), 552–564 (Apr 2011), DOI: 10.1109/TC.2010.82
9. Lebeck, A.R., Fan, X., Zeng, H., Ellis, C.: Power aware page allocation. *ACM SIGOPS Operating Systems Review* 34(5), 105–116 (Dec 2000), DOI: 10.1145/384264.379007
10. Li, S., Chen, K., Ahn, J.H., Brockman, J.B., Jouppi, N.P.: Cacti-p: Architecture-level modeling for SRAM-based structures with advanced leakage reduction techniques. In: *IEEE/ACM International Conference on Computer-Aided Design (ICCAD)*. pp. 694–701. IEEE (Nov 2011), DOI: 10.1109/ICCAD.2011.6105405
11. Micron Technology Inc.: Micron MT40A2G4 data sheet (Oct 2015)
12. Sato, M., Chengguang, H., Komatsu, K., Egawa, R., Takizawa, H., Kobayashi, H.: An energy-efficient dynamic memory address mapping mechanism. In: *IEEE Symposium on Low-Power and High-Speed Chips (COOL Chips XVIII)*. pp. 1–3. Yokohama, Japan (Apr 2015), DOI: 10.1109/CoolChips.2015.7158660
13. Tran, K., Ahn, J.: HBM: Memory solution for high performance processors. In: *MemCon*. Santa Clara, CA, USA (Oct 2014)
14. Udipi, A.N., Muralimanohar, N., Chatterjee, N., Balasubramonian, R., Davis, A., Jouppi, N.P.: Rethinking DRAM design and organization for energy-constrained multi-cores. *SIGARCH Comput. Archit. News* 38(3), 175–186 (Jun 2010), DOI: 10.1145/1816038.1815983
15. Weis, C., Loi, I., Benini, L., Wehn, N.: Exploration and optimization of 3-D integrated DRAM subsystems. *IEEE Transactions on Computer-Aided Design of Integrated Circuits and Systems* 32(4), 597–610 (Apr 2013), DOI: 10.1109/TCAD.2012.2235125
16. Wilkes, M.V.: The memory gap and the future of high performance memories. *SIGARCH Comput. Archit. News* 29(1), 2–7 (Mar 2001), DOI: 10.1145/373574.373576
17. Wu, D., He, B., Tang, X., Xu, J., Guo, M.: RAMZzz: Rank-aware DRAM power management with dynamic migrations and demotions. In: *The International Conference on High Performance Computing, Networking, Storage and Analysis*. pp. 32:1–32:11. Los Alamitos, CA, USA (Nov 2012), DOI: 10.5555/2388996.2389040
18. Wulf, W.A., McKee, S.A.: Hitting the memory wall: Implications of the obvious. *ACM SIGARCH Computer Architecture News* 23, 20–24 (Mar 1995), DOI: 10.1145/216585.216588
19. Yamada, Y.: Vector engine processor of NECs brand-new supercomputer SX-Aurora TSUBASA. In: *HotChips: A Symposium on High Performance Chips*. Cupertino, CA, USA (Aug 2018), [https://www.hotchips.org/hc30/2conf/2.14\\_NEC\\_vector\\_NEC\\_SXAurora\\_TSUBASA\\_HotChips30\\_finalb.pdf](https://www.hotchips.org/hc30/2conf/2.14_NEC_vector_NEC_SXAurora_TSUBASA_HotChips30_finalb.pdf)